LAWRENCE
LIVERMORE
NATIONAL
LABORATORY

UCRL-JRNL-219533

Calculation of the Slip System Activity in Deformed Zinc Single Crystals Using Digital 3-D Image Correlation Data

J.N. Florando, M. Rhee, A. Arsenlis, M.M. LeBlanc, D.H. Lassila

March 6, 2006

Philosophical Magazine Letters

Calculation of the Slip System Activity in Deformed Zinc Single Crystals Using Digital 3-D Image Correlation Data

J.N. FLORANDO*, M.RHEE, A. ARSENLIS, M.M. LEBLANC, AND D.H. LASSILA
Lawrence Livermore National Laboratory, Livermore, CA 94550, U.S.A.

A 3-D image correlation system, which measures the full-field displacements in 3 dimensions, has been used to experimentally determine the full deformation gradient matrix for two zinc single crystals. Based on the image correlation data, the slip system activity for the two crystals has been calculated. The results of the calculation show that for one crystal, only the primary slip system is active, which is consistent with traditional theory. The other crystal however, shows appreciable deformation on slip systems other than the primary. An analysis has been conducted which confirms the experimental observation that these other slip system deform in such a manner that the net result is slip which is approximately one third the magnitude and directly orthogonal to the primary system.

Keywords: Image correlation, single crystal, slip system activity, compression

1. Introduction

The critical resolved shear stress law, proposed by Schmid and Boas [1], relates the slip activity for a given slip system to the resolved shear stress. Since then, there have been studies that have attempted to quantify and relate the slip activity to the macroscopic shape change of a single crystal sample. Chin et. al [2], established a method to compute the slip system activity based on the experimental deformation gradient matrix. Johnson [3], refined this method and applied it to copper single crystals deformed in tension, and recently, Basinski and Basinski [4] performed a detailed study applying the mathematical method developed by Chin to many different orientations of Cu single crystals. While the methodology used in these studies is very powerful, the accuracy of these studies is dependent upon the experimentally measured deformation gradient matrix.

Taylor and Elam [5], in their pioneering work on crystal plasticity, measured the orientation and shape change in Al crystals under deformation. While in principle, this method can measure the deformation gradient matrix, the experimental techniques available at the time did not allow an accurate calculation of the activity on secondary slip systems [4]. Basinski and Basinski, in a recent study [4], used a method that accurately determines the orientation and global shape change of the sample, however, the calculated deformation gradient is averaged over a fairly large area (2cm by 2cm), and the samples are subjected to relatively large strains (5- 8%) before the first shape change is measured.

Recently, a digital 3-D image correlation technique has been used to study the deformation of single crystals [6]. Since this technique measures the displacements of the sample in three dimensions, the complete displacement gradient matrix can be determined. This technique is also full-field, meaning, the local gradients can be measured in specific regions to account for the inherent inhomogenities that occur during the deformation of single crystals.

The purpose of this letter is to show how the deformation gradient matrix measured experimentally using the image correlation technique, is applied to an analysis to calculate the slip system activity in deformed zinc single crystals.

2. Procedure

Two high purity zinc single crystals with a purity of 99.98% were grown using the Bridgman technique by Accumet Inc., Briarcliff Manor, NY. Tests samples with dimensions 5 mm by 5mm wide and 15 mm tall were fabricated out of the crystals. One zinc crystal sample, which was taken out of a pristine crystal, has an orientation with the $[8\ \overline{11}\ 3\ \overline{30}]$ direction pointing out of the z direction. Another sample was taken from a crystal that was mechanically bent to introduce a small amount of cold work and then annealed at room temperature for several weeks. This sample is oriented such that the $[\bar{2}\ 4\ \bar{2}\ 3]$ direction is pointing along the z-direction as shown in figure 1.

The samples were compressed using the “6 Degrees of Freedom” testing apparatus [7], which allows the sample to deform virtually unconstrained in 6 directions. The full-

field deformation of the sample was measured using the Aramis 3-D image correlation system. While the details of the image correlation technique are presented elsewhere [8, 9], the premise behind image correlation is that images of a stochastic pattern on the sample (typically black dots on a white background for the highest contrast) are recorded with a CCD camera during deformation. The images are then compared, and the relative movement and shape change of the dots in relation to one another gives local displacements that can be used to calculate strain. By using a pair of cameras, both in-plane and out-of-plane displacements can be measured. While photos of the four faces were taken before and after the test, two pairs of cameras were used to take pictures of two faces real time.

An example of the image correlation strain maps for the samples in the two orientations are also shown in figure 1. The maps show the inhomogenities that can occur in the deformation of single crystals. To extract the displacement gradient matrix from the image correlation maps, the following procedure is used. For each face, 5 horizontal (x') and 5 vertical (y') lines are drawn in the area of interest, where x' and y' are the local x and y coordinates. For the x', y', and z' displacements, as shown in figure 2, the displacement along a particular axis is measured, and the change in displacement as a function of the line (dui/dj) is calculated and averaged between the 5 lines. The area where the displacement gradient is measured is based upon the region of interest from the strain maps. For instance, for the pristine zinc sample, the displacement gradient was measured in the area where the largest deformation occurred since that corresponds to the primary slip plane. For the 'cold worked and annealed' zinc sample, the area in the middle of the sample was chosen to capture the intersection of both the primary and secondary slip.

3. Calculation of slip system activity

Following the analysis by Chin et. al [2], and Johnson [3], the calculation of the slip system activity in the zinc crystals can be calculated from the experimental displacement gradient matrix.

The displacement gradient matrix, **U**, can be expressed as

$$\mathbf{U_{ij}} = \frac{\mathrm{du_i}}{\mathrm{dx_j}}, \qquad (1)$$

where i and j are taken along the x, y, and z axes in the global laboratory coordinate system. The nine components of the displacement gradient matrix completely specify the deformation of the sample. For a given slip system, the Schmid tensor **S** can be expressed as

$$\mathbf{S_{ij}} = \boldsymbol{b_i n_j}, \qquad (2)$$

where ***b*** is the unit vector along the slip direction (Burgers vector), and ***n*** is the unit vector normal to the slip plane. If more than one slip system is active then the total displacement gradient matrix, using the small strain approximation [3], can be expressed as

$$\mathbf{U_{total}} = \sum_{\alpha=1}^{k} \gamma^{\alpha} \mathbf{S}^{\alpha}{}_{\mathbf{ij}}, \qquad (3)$$

where γ^{α} is the amount of slip that occurs for the slip system α. This equation however, requires that the amount of slip activity of each slip system be known. Typically it is this quantity, gamma, that is unknown and that must be calculated from the experimentally measured $\mathbf{U}_{\mathrm{total}}$. Solving for the gammas gives k number of equations. There are nine components in **U**, however, since there is no volume change during plastic deformation, $\frac{\mathrm{du_1}}{\mathrm{dx_1}} + \frac{\mathrm{du_2}}{\mathrm{dx_2}} + \frac{\mathrm{du_3}}{\mathrm{dx_3}} = 0$, only eight of these components are linearly independent. Eqn [3] can then be rewritten as

$$\mathbf{U_{exp}} = \mathbf{Mg}, \qquad (4)$$

where $\mathbf{U}_{exp}$ is an 8x1 matrix that contains the components of the experimentally measured displacement gradient matrix, **M** is an 8x8 matrix that contains the 8 independent components of the Schmid tensor for each particular slip system, and **g** is an 8 x 1 matrix that contains the activity for each slip system. Solving for **g** gives

$$\mathbf{g} = \mathbf{M}^{-1}\mathbf{U}_{\mathbf{exp}}. \qquad (5)$$

The main assumption in applying this analysis to the experimental data is that the orientation of the sample relative to the loading axis does not change significantly during the test. The 6DOF was specifically designed to minimize this rotation, and x-ray analysis confirms that there is no rotation greater than the resolution of our x-ray analysis, which is ± 0.5 degrees.

Equation 5 can be applied to solve for the slip system activity for the deformed zinc samples using the following modifications. In order to use the analysis described above, the traditional 4-index Miller indices used to describe crystallographic directions in hexagonal crystal systems, must be converted to a 3-index system compatible with an orthogonal set of axes. The conversion from the 4-index notation [*h k i l*] to the 3-index notation [H K L] in hexagonal systems can be calculated using:

$$\begin{aligned} \mathrm{H} &= 2h + k \\ \mathrm{K} &= h + 2k \\ \mathrm{L} &= l \end{aligned} \qquad (6)$$

An orientation represented in the hexagonal system can be represented in an orthogonal set of axes from [10]

$$\begin{bmatrix} \mathrm{U} \\ \mathrm{V} \\ \mathrm{W} \end{bmatrix} = \begin{bmatrix} a_o \sin 60^o & 0 & 0 \\ -a_o \cos 60^o & a_o & 0 \\ 0 & 0 & c_o \end{bmatrix} \begin{bmatrix} \mathrm{H} \\ \mathrm{K} \\ \mathrm{L} \end{bmatrix}, \qquad (7)$$

where a_o and c_o are the lattice parameters for the hexagonal system., and for zinc a_o= 2..6649 Å, and c_o= 4.9468 Å.

For zinc crystals, slip mainly occurs in the closed-packed basal plane {0001} along the closed packed $<1\,\bar{2}\,1\,0>$ directions. Previous work [11, 12] has shown that non-basal slip can also occur along the 2nd order pyramidal slip systems $\{1\,1\,\bar{2}\,2\}<1\,1\,\bar{2}\,3>$. For the basal (0001) plane there are two linearly independent $<1\,\bar{2}\,1\,0>$ directions, and there are five linearly independent $<1\,1\,\bar{2}\,3>$ directions for the 2nd order pyramidal planes $\{1\,1\,\bar{2}\,2\}$ planes, giving a total of 7 linearly independent slip systems. As previously mentioned, equation 5 allows for eight independent slip systems to be solved simultaneously. While it is always possible to add another set of slip systems, a review of the literature [11-13] has not indicated activity on any additional slip systems in zinc. Instead of artificially adding a slip system, two of the components of **U** can be combined to give 7 independent equations. The new **U** can be shown as

$$\mathbf{U}_{\alpha} = \begin{bmatrix} du_1/dx_1 \\ 1/2(du_1/dx_2 + du_2/dx_1) \\ du_1/dx_3 \\ du_2/dx_2 \\ du_2/dx_3 \\ du_3/dx_1 \\ du_3/dx_2 \end{bmatrix}. \qquad (8)$$

The average of the global du_1/d_2 and du_2/d_1 displacements gradients gives the global ε_{12} strain. These particular displacement gradients were chosen to average because they represent shear deformation that occurs normal to the loading direction, and are expected to be small in comparison to the other shear components. In addition, the measured

values were approaching the noise level of the system for the measurement of the displacement gradients (0.0001), and by averaging the two components; the error associated with their measurement was reduced.

Since there are nine possible slip systems (only 7 are linearly independent) a program has been written which iterates through the possible combinations of slip systems and calculates the corresponding slip system activity. The Burgers vector and slip plane normal for each slip system is chosen to be consistent with a positive shear stress due to a compressive load on the sample. For example, figure 3a shows a schematic of a slip system in a crystal subjected to a compressive load. In this case, a positive resolved shear stress is defined as heading in the + x direction on the +z face as shown in figure 3b. Slip system work can be defined as,

$$W^{\alpha} = \int \gamma^{\alpha} \mathrm{d}\tau \qquad (9)$$

where γ^{α} is the slip system activity and τ is the resolved shear stress. In order to be consistent with positive work, the Burgers vector and slip plane normal vector much be chosen to produce a positive shear strain that is consistent with the definition of a positive shear stress. Table 1 lists the slip systems for both zinc samples that are consistent with positive work under compression loading. If the sample were subjected to tensile loading instead of compression, then for a given the slip system, changing the sign of the Burgers vector would satisfy the positive work criteria for tension.

4. Results and discussion

As seen in figure 1, the pristine zinc sample shows a large band of deformation occurring at approximately 18 degrees to the horizontal, and this correspond to the trace of the primary slip system $(0\,0\,0\,\bar{1})\ [\bar{1}\,2\,\bar{1}\,0]$ on this face. The slip system activity was calculated using the methodology described above. For the final stage, after the sample was unloaded, the results, Table 2, show that there are multiple solutions that are consistent with positive work under compression loading. The common characteristic between all of them however, is that nearly all of the activity (> 90%) is occurring along

the primary slip system. It should be noted that for this analysis, the error bar associated with the calculation of the slip system activity is ± 0.05%. A plot of the slip system activity as a function of axial strain for one of the solutions is shown in figure 4a. It clearly shows that throughout the experiment, the sample is mainly deforming on the primary slip system, in accordance with traditional theory [1].

While the pristine zinc deforms in a manner according to Schmid's law, the "cold worked and annealed" sample shows much different behavior. In the image correlation results, shown in figure 1, there appears to be two bands of deformation that occur 45 degrees from the horizontal and 90 degrees apart. The calculated slip system activity for this sample is shown in Table 3. For the final stage of this sample, there are only two solutions that are consistent with the compression loading. In comparing the two solutions, the first solution has a lower sum of the gammas, possibly signifying a lower energy configuration. Also, the second solution shows that the next two largest gammas after the primary occur along slip systems that have nearly zero resolve shear stresses on them. Since this is unlikely to occur, the first solution seems to be the most plausible. A plot of the slip system activity versus axial strain using the systems in the first solution is shown in figure 4b. It clearly shows that while the primary system is the most active, there are other slip systems which also have a large contribution to the overall behavior. The fact that the 2^{nd} order pyramidal systems are active is rather surprising because the critical resolved shear stress for these systems is an order of magnitude greater than for the primary system [12]. The pre-bending of the sample, therefore, must have activated sources on these pyramidal planes. In addition, the slip activity on these slip systems combine in such a manner as to produce a net slip that is directly orthogonal to the primary slip system.

5. Calculation of the maximum displacement gradient

Another way to characterize the deformed sample using the displacement gradient matrix is to find the orientation that corresponds to the maximum displacement gradient. This calculation is similar to finding the principal stress and strain using methods such as Mohr's circle. Those equations do not apply in this situation however, because unlike the strain tensor, the displacement gradient tensor is not symmetric.

Our methodology to calculate the maximum displacement gradient is to rotate the experimentally measured $\mathbf{U_{exp}}$ through space, and calculate the corresponding **U'** for that given rotation, keeping track of the maximum value. The rotation of $\mathbf{U_{exp}}$ can be described using the three Euler angles, which also maintains the three orthogonal right-hand axes. If the original axes can be represented by x, y, and z, then the total transform matrix can then be described as

$$\mathbf{T} = \mathbf{R_z}(\alpha)\, \mathbf{R_{y'}}(\beta)\, \mathbf{R_{z''}}(\gamma). \qquad (10)$$

where **R** is a rotation matrix, α is the angle of rotation around z, β is the angle of rotation around the y' axis, and γ is the angle of rotation around the z'' axis. The rotated displacement gradient matrix can then be calculated using

$$\mathbf{U'} = \mathbf{T}\, \mathbf{U_{exp}}\, \mathbf{T}^{T}. \qquad (11)$$

To find the rotation where the maximum displacement gradient value occurs, the three Euler angles were incremented in steps of 0.1 degrees from 0 to 90 degrees. Using this methodology, for a sample where only primary slip occurs, the axes where the maximum displacement gradient value occurs should correspond to the primary system. An alternative case where the axes would line up with the primary system is if the slip occurred on the primary, and the net slip from other slip systems occurs at exactly 90 degrees to the primary. One can imagine that if slip occurred on multiple systems where the net secondary slip was not 90 degrees to the primary, then the maximum would occur at some orientation in between the primary and the net direction from the other slip systems.

For the pristine zinc sample, the results of the maximum displacement gradient matrix analysis, Table 4, shows that the maximum value of 0.0313 occurs in the x' direction along the z' axis, and all other values in the rotated matrix are essentially zero.. Plotting the x' and z' vectors in relation to primary Burgers vector $[\bar{1}\ 2\ \bar{1}\ 0]$ and slip plane normal $[0\,0\,0\,\bar{1}]$, figure 4a, shows that these axis correspond to the primary system. It

should also be noted that the maximum value is equal to the slip activity calculated using the slip system analysis.

For the "cold worked and annealed" sample, the rotation of the displacement gradient matrix gives the solution shown in Table 5. While the maximum value of 0.063 does occur when the x' and z' axes are close to the primary slip system, figure 4b, there is also an appreciable component (nearly 1/3 of the primary) in the orthogonal direction, signifying that slip is occurring 90 degrees to the primary. This result confirms the results seen in figure 1b, and is consistent with the values calculated in the slip system analysis, and those experimentally measured using the image correlation system [7]. The fact that slip is exactly 90 degrees to the primary system suggests that there is a minimum energy configuration associated with forming dislocation structures that occur along both the primary and orthogonal to the primary system. This configuration occurs even though there is no slip system directly orthogonal to the primary system.

6. Conclusions

Using data from a 3-D image correlation technique to measure the full displacement gradient matrix, an analysis has been performed to calculate the slip system activity for two zinc single crystals. The results show that a pristine zinc sample deformed in a manner consistent with Schmid's Law. The "cold worked and annealed" sample, however, did not deform according to traditional theory, and the results show that appreciable deformation occurred along slip systems other than the primary. In addition, the sum of the other slip systems was found to be exactly orthogonal to the primary system. The exact nature of the orthogonal slip is unknown, but it is suspected that this slip occurs to minimize the energy associated with a build up of internal stresses during deformation.

7. Acknowledgements

The authors would like to thank Dr. John Hirth for his comments during a critical reading of an early draft of this manuscript. The authors would also like to thank Ann Bliss for performing Laue x-ray diffraction to determine the crystallographic orientations. This work was funded by the LLNL "Dynamics of Metals" and Laboratory Directed Research

and Development programs. This work was performed under the auspices of the U.S. Department of Energy by the University of California, Lawrence Livermore National Laboratory under Contract W-7405-ENG-48.

8. References

[1] E. Schmid and I.W. Boas, *Plasticity of Crystals*, London: Chapman and Hall (1950).
[2] G.Y. Chin, R.N. Thurston, and E.A. Nesbitt, Trans metall. Soc. AIME, 236, 69 (1966).
[3] L. Johnson, Trans metall. Soc. AIME, 245, 275 (1969).
[4] Z.S. Basinski and S.J. Basinski, Phil. Mag., 84(3-5), 213-251 (2004).
[5] G.I. Taylor and C.F. Elam, Roy. Soc. Proc. A, 102A, 643 (1923).
[6] M.M. LeBlanc, et al., Exp. Tech., 30 (2006).
[7] D.H. Lassila, M.M. LeBlanc, and J.N. Florando, Met. and Mat. Trans. A., (sub. 2006).
[8] T. Schmidt, J. Tyson, and K. Galanulis, Exp. Tech., 27(4), 22-26 (2003).
[9] W.H. Peters and W.F. Ranson, Opt. Eng., 21(3), 427-431 (1982).
[10] D. McKie and C. McKie, *Essential of Crystallography*, Oxford: Blackwell (1986).
[11] P.B. Price, in *Electron Microscopy and Strength of Crystals*, edited by G. Thomas and J. Washburn, Interscience, New York (1963).
[12] H. Tonda and S. Ando, Met. and Mat. Trans. A., 33A, 831-836 (2002).
[13] R.L. Bell and R.W. Cahn, Proc. Roy. Soc., A239, 494 (1957).

List of figure captions

Figure 1-Image correlation strain maps a)Zinc crystal showing slip only on the primary system (Schmid's Law) b)Zinc crystal showing slip on the primary system, and slip orthogonal to the primary system.

Figure 2-Displacement maps of the "B" side of the pristine zinc sample. The displacement gradients are calculated by taking the slope of the displacement as a function of the axes (x' or y'). The slopes are calculated for 5 lines and averaged.

Figure 3- a) Schematic of a slip system in a sample under compression loading b) Schematic representation of a positive shear stress on a slip system under compression loading and the corresponding direction of the Burgers vector that is consistent with positive work.

Figure 4-Results of slip system calculation a) for the pristine sample showing slip only on the primary slip system b) for the "cold worked and annealed" sample showing slip on the primary and on additional slip systems.

Figure 5- Axes of the maximum displacement gradient in relation to the primary Burgers vector $[\bar{1}2\bar{1}0]$ and the slip plane normal $[000\bar{1}]$ a) for the pristine zinc sample b) for the "cold work and annealed" sample. In both cases the rotated axes are in close agreement with the primary system. For these plots, the y' axis is projected onto the $\hat{b} - \hat{n}$ plane, and no out of plane rotation would yield a point at the intersection of the two axis.

Tables

Table 1: Slip systems consist with positive work for compression loading on the sample

Slip system ID	For the pristine zinc Slip systems with positive work (plane) [Burgers vector]	For the "cold worked and annealed" zinc Slip systems with positive work (plane) [Burgers vector]
ss1	$(000\bar{1})$ $[\bar{1}2\bar{1}0]$	(0001) $[1\bar{2}10]$
ss2	$(000\bar{1})$ $[11\bar{2}0]$	(0001) $[\bar{1}\bar{1}20]$
ss3	$(000\bar{1})$ $[\bar{2}110]$	(0001) $[2\bar{1}\bar{1}0]$
ss4	$(\bar{1}2\bar{1}\bar{2})$ $[\bar{1}2\bar{1}3]$	$(1\bar{2}12)$ $[\bar{1}2\bar{1}3]$
ss5	$(1\bar{2}1\bar{2})$ $[1\bar{2}13]$	$(\bar{1}2\bar{1}2)$ $[\bar{1}2\bar{1}\bar{3}]$
ss6	$(\bar{1}\bar{1}2\bar{2})$ $[\bar{1}\bar{1}23]$	$(11\bar{2}2)$ $[11\bar{2}\bar{3}]$
ss7	$(2\bar{1}\bar{1}\bar{2})$ $[2\bar{1}\bar{1}3]$	$(\bar{2}112)$ $[\bar{2}11\bar{3}]$
ss8	$(\bar{2}11\bar{2})$ $[\bar{2}113]$	$(2\bar{1}\bar{1}2)$ $[\bar{2}113]$
ss9	$(11\bar{2}\bar{2})$ $[11\bar{2}3]$	$(\bar{1}\bar{1}22)$ $[11\bar{2}3]$

Table 2: Slip system activity solutions for the pristine zinc sample

Slip system	$(000\bar{1})$ $[\bar{1}2\bar{1}0]$	$(000\bar{1})$ $[\bar{2}110]$	$(\bar{1}2\bar{1}\bar{2})$ $[\bar{1}2\bar{1}3]$	$(1\bar{2}1\bar{2})$ $[1\bar{2}13]$	$(\bar{1}\bar{1}2\bar{2})$ $[\bar{1}\bar{1}23]$	$(2\bar{1}\bar{1}\bar{2})$ $[2\bar{1}\bar{1}3]$	$(\bar{2}11\bar{2})$ $[\bar{2}113]$	$(11\bar{2}\bar{2})$ $[11\bar{2}3]$
Solution 1	0.031	0.001	0.000	0.001	0.000	0.000		0.001
Solution 2	0.031	0.001	0.001	0.001	0.000		0.000	0.000
Solution 3	0.031	0.001	0.000	0.001		0.000	0.000	0.000

Table 3: Slip system activity solutions for the "cold worked and annealed" zinc sample

Slip system	(0001) $[1\bar{2}10]$	$(000\bar{1})$ $[2\bar{1}\bar{1}0]$	$(1\bar{2}12)$ $[\bar{1}2\bar{1}3]$	$(\bar{1}2\bar{1}2)$ $[\bar{1}2\bar{1}\bar{3}]$	$(11\bar{2}2)$ $[11\bar{2}\bar{3}]$	$(\bar{2}112)$ $[\bar{2}11\bar{3}]$	$(2\bar{1}\bar{1}2)$ $[\bar{2}113]$	$(\bar{1}\bar{1}22)$ $[11\bar{2}3]$
Solution 1	0.067	0.004	0.018	0.009	0.003		0.002	0.003
Solution 2	0.067	0.004	0.009		0.012	0.009	0.011	0.012

Table 4: Rotated maximum displacement gradient solution for the pristine zinc where $\alpha = 85.6^{o}$, $\beta = 17.5^{o}$, and $\gamma = 13.1^{o}$.

$du_{x'}/d_{x'}$	$du_{x'}/d_{y'}$	$du_{x'}/d_{z'}$	$du_{y'}/d_{x'}$	$du_{y'}/d_{y'}$	$du_{y'}/d_{z'}$	$du_{z'}/d_{x'}$	$du_{z'}/d_{y'}$	$du_{z'}/d_{z'}$
0.0000	0.0000	**0.031**	-0.001	0.000	0.0000	0.0000	0.0000	0.000

Table 5: Rotated maximum displacement gradient solution for the "cold worked and annealed" zinc where $\alpha = 1.5^{o}$, $\beta = 44.2^{o}$, and $\gamma = 1.1^{o}$.

$du_{x'}/d_{x'}$	$du_{x'}/d_{y'}$	$du_{x'}/d_{z'}$	$du_{y'}/d_{x'}$	$du_{y'}/d_{y'}$	$du_{y'}/d_{z'}$	$du_{z'}/d_{x'}$	$du_{z'}/d_{y'}$	$du_{z'}/d_{z'}$
0.001	0.000	**0.063**	-0.002	0.000	0.000	**0.024**	-0.002	0.001

Figures

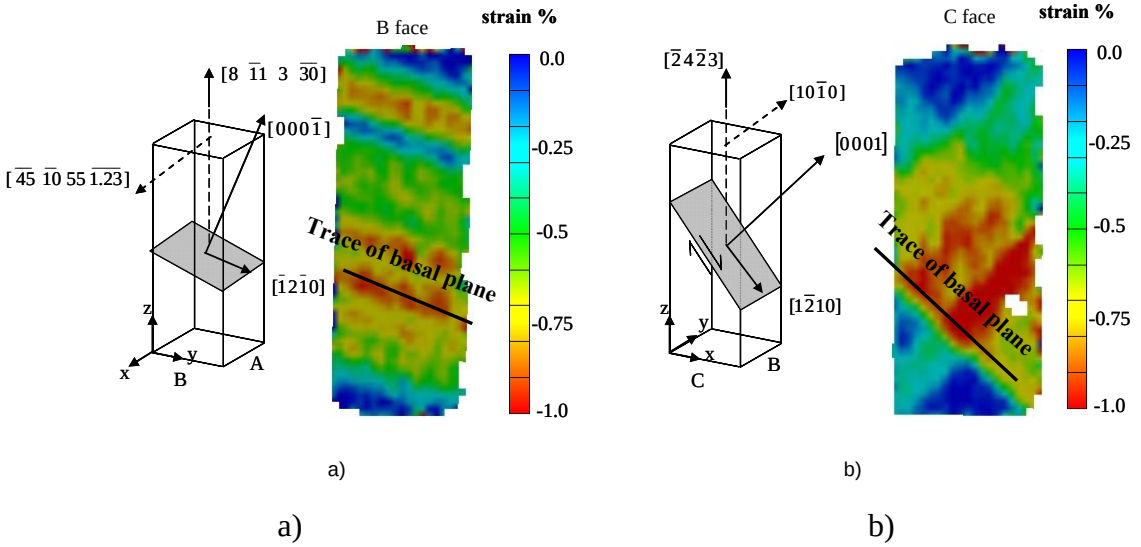

a) b)

Figure 1-Image correlation strain maps a)Zinc crystal showing slip only on the primary system (Schmid's Law) b)Zinc crystal showing slip on the primary system, and slip orthogonal to the primary system.

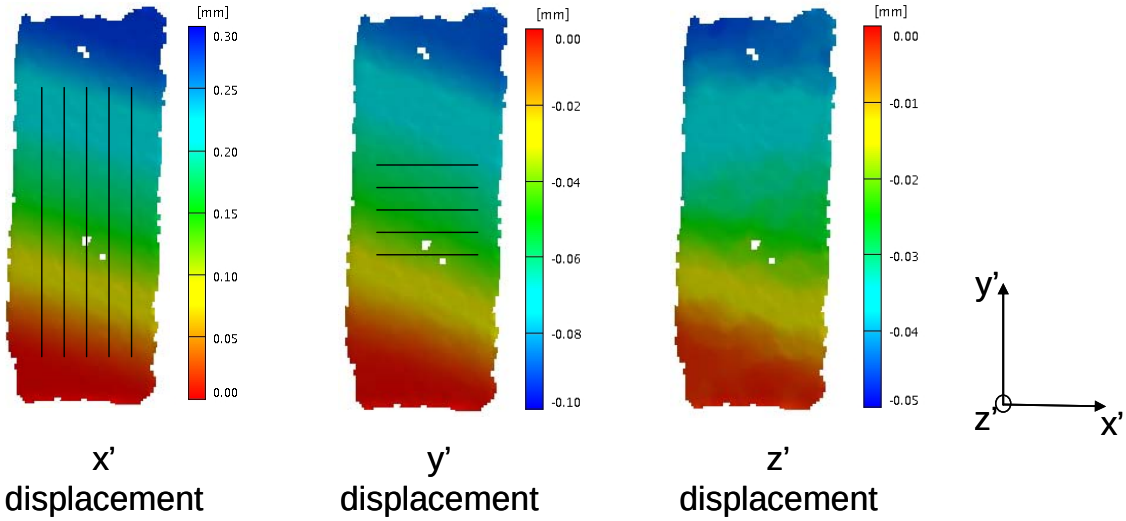

Figure 2-Displacement maps of the "B" side of the pristine zinc sample. The displacement gradients are calculated by taking the slope of the displacement as a function of the axes (x' or y'). The slopes are calculated for 5 lines and averaged.

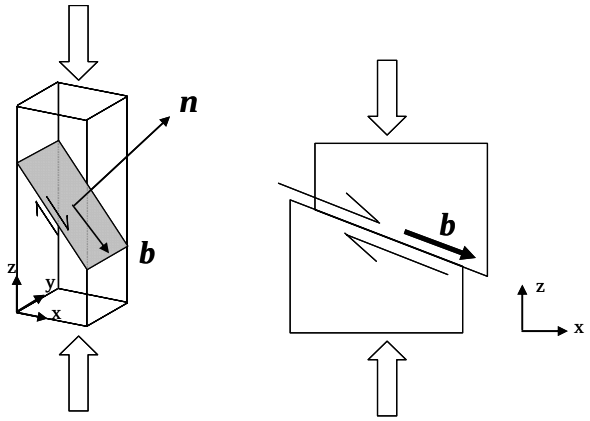

a) b)

Figure 3- a) Schematic of a slip system in a sample under compression loading b) Schematic representation of a positive shear stress on a slip system under compression loading and the corresponding direction of the Burgers vector that is consistent with positive work.

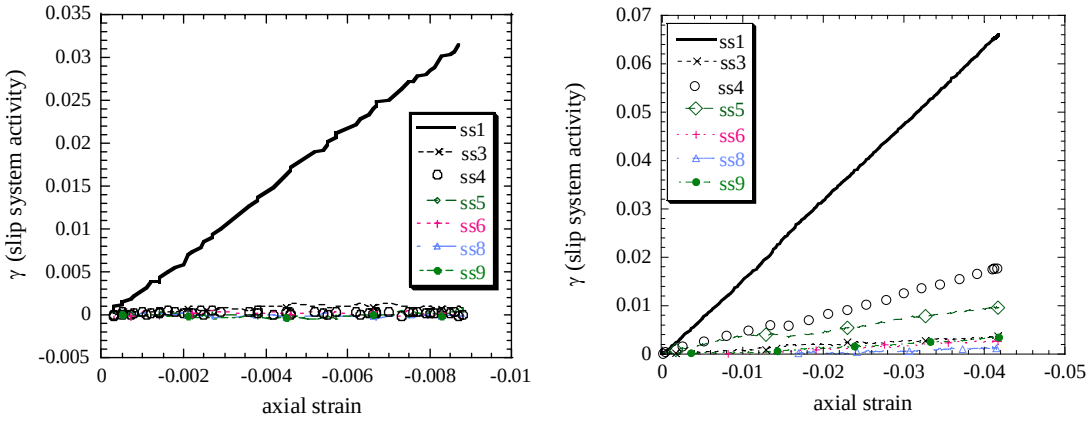

a) b)

Figure 4-Results of slip system calculation a) for the pristine sample showing slip only on the primary slip system b) for the "cold worked and annealed" sample showing slip on the primary and on additional slip systems.

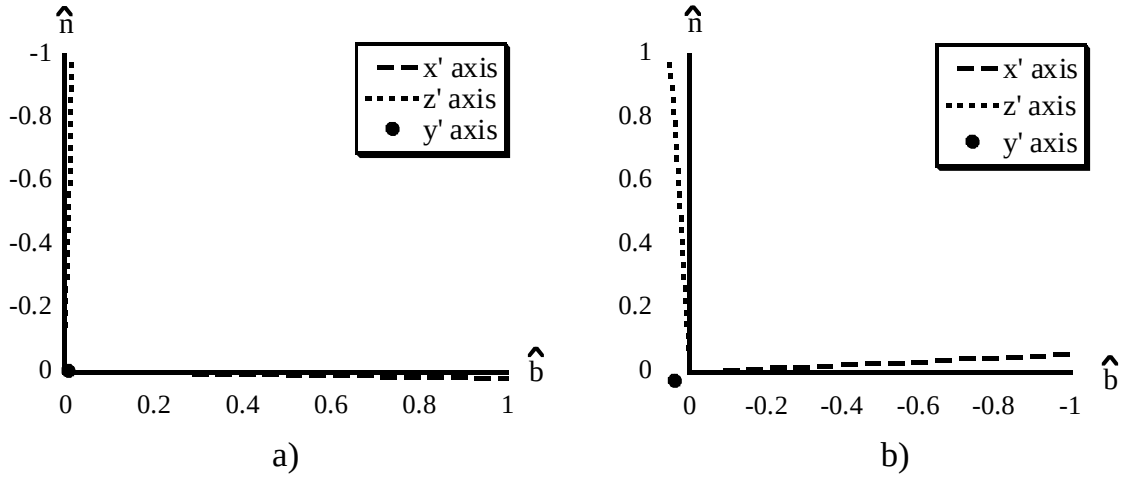

Figure 5- Axes of the maximum displacement gradient in relation to the primary Burgers vector $[\bar{1}2\bar{1}0]$ and the slip plane normal $[000\bar{1}]$ a) for the pristine zinc sample b) for the "cold work and annealed" sample. In both cases the rotated axes are in close agreement with the primary system. For these plots, the y' axis is projected onto the $\hat{b} - \hat{n}$ plane, and no out of plane rotation would yield a point at the intersection of the two axis.